EXPERIMENTAL REVIEW OF THE WELDING METALLURGY OF HIGH-STRENGTH ALUMINIUM ALLOY 7025-T6

M. OLABODE, P. KAH and **J. MARTIKAINEN**
Lappeenranta University of Technology, Lappeenranta, Finland

In this review, various aspects such as designations, definitions, applications, properties and weldability of high-strength aluminium alloys are presented. The effect of heat input on microstructure and hardness of the 7025-T6 alloy welded joints is studied. It is shown that at constant heat input the welding speed had no effect on the weld hardness. Thus, limiting heat input in welds on high-strength aluminium alloys is important to preserve their mechanical properties.

Keywords: *high-strength aluminium alloys, alloy 7025-T6, pulsed MIG welding, heat input, Vickers hardness, welding metallurgy*

Light welded metal structures are in high demand, and the market keeps growing along with societal needs. The diversification of aluminium structures also continues to grow. Welding is an important process in producing these structures. The fusion welding of high-strength aluminium alloys (HSA) using pulsed MIG method involves heat input and is, thus, challenging but accomplishable if proper care is taken to understand the nature and behaviour of HSA being welded. A number of studies [1–3] have shown that earlier technologies available for welding HSA present poor weldability due to the presence of copper in the alloy. However, new technologies like pulsed MIG welding, pulsed TIG welding and friction stir welding (FSW) can be effectively to compared with conventional fusion methods. FSW proved to be presently the most acceptable process as it allows obtaining important metallurgical advantages, for example, no solidification and liquation cracking, compared with fusion welding [4]. Based on literature review, this paper outlines the definitions, properties, applications, weldability, welding defects of HSA and studies their weldability with a focus on the effect of heat input on welding metallurgy using the pulsed MIG process. This study adopts both a literature review of HSA and an experimental study of 7025-T6 alloy welded by robotised pulsed MIG method. In addition, the effect of heat input and welding speed as welding parameters on welding metallurgy of HSA are presented. It was found that the grains reduce in size as heat input decreases, and welding speed had no effect on the hardness across the weld if heat input was kept constant. The hardness of HSA joints lower in the HAZ than in the parent metal. This study is of significance as there are limited studies available about the welding metallurgy of the 7025-T6 alloy.

Alloy designation. Aluminium alloys are grouped into cast and wrought ones and are identified with a four digit number system. Cast alloy designations are similar to those of wrought alloys but with a decimal between the third and fourth digit (123.0). The second part of the designation is the temper which accounts for the fabrication process. When the second part starts with T, e.g. T6, it means that the alloy was thermally treated. The numbers show the type of the treatment and other consequent mechanical treatment, namely T6 shows that the alloy is solution heat-treated and artificially aged [5]. In alloy designations F denotes as fabricated and O — annealed. An additional suffix indicates the specific heat treatment. H denotes strain-hardened (cold-worked) and it is always followed by at least two digits to identify the level of cold-working and other heat treatments that have been carried out to attain the required mechanical properties. W denotes solution heat-treated, it is followed by a time indicating the natural ageing period, e.g. W 1 h. T denotes thermally treated and is always followed by one or more numbers to identify the specific heat treatment [4].

The full designation therefore has two parts which specify the chemistry and the fabrication history, e.g. in 7025-T6, 7025 specifies the chemistry while T6 — the fabrication. Aluminium is classified based on the chemical composition. The classification is mainly in two categories based on the type of production which are wrought aluminium alloys (fabricated alloys) and cast aluminium alloys. Others can be categorised on the basis of strain hardening possibility or heat treatment [6]. The wrought aluminium category is large because aluminium can be formed to shapes by virtually any known process including extruding, drawing, forging, rolling etc. Wrought alloys need to be ductile to aid fabrication, whereas cast aluminium alloys need to be fluid in nature to aid castability [7]. Cast aluminium alloys are identified with four digits in their classification. A decimal point separates the third and fourth digit. The first digit indicates the alloy group which is based on the major alloying element (Table 1) [8]. The next two digits denote the aluminium alloy itself or the purity of the alloy. In lxx.x series

Table 1. Cast aluminium alloy classification [6–9]

Series	Alloying elements	Content, %	Tensile strength, MPa	Series average value, MPa
1xx.x	Al	Min 99.0		
2xx.x	Cu	4.0–4.6	145–476	302
3xx.x	Si	5–17	159–359	249
	With added Cu and/or Mg	5–17	159–359	249
4xx.x	Si	5–12	131–296	187
5xx.x	Mg	4–10	138–331	232
7xx.x	Zi	6.2–7.5	241	241
8xx.x	Sn	–	138–221	163
9xx.x	Others	–	–	–

alloys, these two digits denote the purity in percentages. For example, 150.0 show the minimum 99.5 % purity of the aluminium alloy. In the groups 2xx.x–9xx.x series, the two digits signify the different alloys present in the group. The last digit signifies how the product is formed. For example, 0 denotes casting, and 1 or 2 — ingot based on what chemical composition the ingot has.

Further modifications from the original cast aluminium alloy groups are identified by adding a serial letter in front of the numerical denotations. The serial letters are assigned in alphabetical order starting with A but omitting I, O, Q and X [8]. X is left out with experimental alloys.

Wrought alloys are given four digits. The first one represents the alloy group which is based on the major alloying element (Table 2). The second digit tells how the alloy has been modified or the limits of impurity. 0 in the second digit denotes an original alloy. Numbers 1–9 signify the different alloy modifications with slight variation in their compositions. In the 1xxx series the second number denotes the modifications in impurity limits: 0 implies that the alloy has a natural impurity limit, 1–9 imply that special control has been carried out on one or more impurities or alloying element. The last two numbers represent the purity of the alloy [6].

In the 1xxx series the last two numbers signify the alloy level of purity. For example, 1070 or 1170 implies that at least 99.7 % Al is present in the alloy, 1050 or 1250 — no less than 99.5 % Al, and 1100 or 1200 — at least 99.0 % Al. For all the other series of aluminium alloys (2xxx–8xxx) the last two numbers have no special significance but are used to identify alloys in the group [6, 8].

High-strength and ultra high-strength aluminium alloys. Aluminium alloys with at least 300 MPa yield strength are regarded to be HSA, whereas ultra high-strength aluminium alloys (UHSA) are those with yield strength of 400 MPa or more. HSA and UHSA are generally included in the 2xxx, 7xxx, and 8xxx series. There are no strict rules as to what series HSA and UHSA belong to. For example, two alloys can have significantly different yield strengths within the same series. To be exact, the HSA and UHSA can be classified only specifically to certain alloys in the series. For generality purpose, however, an average range of the series yield strength is used to identify HSA and UHSA (see Table 2).

Properties and applications of HSA and UHSA Series. The 2xxx series includes the Al–Cu alloys. The major characteristics of the 2xxx series are heat treatability, high strength both at room and elevated temperatures, and high tensile strength range of 68.9–520 MPa [9, 10]. The alloys can be joined mechani-

Table 2. Wrought aluminium alloy classification [6, 8, 9]

Series	Alloying elements	Content, %	Tensile strength, MPa	Series average value, MPa
1xxx	Al	Min 99.0	10.0–165	94.4
2xxx	Cu	1.9–6.8	68.9–520	303
3xxx	Mn	0.3–1.5	41.4–285	163
4xxx	Si	3.6–13.5	70.0–393	275
5xxx	Mg	0.5–5.5	40.0–435	194
6xxx	Mg and Si	0.4–1.5	40.0–435	241
	Si	0.2–1.7	40.0–435	241
7xxx	Zn	1.0–8.2	80.0–725	399
8xxx	Others	–	110–515	365

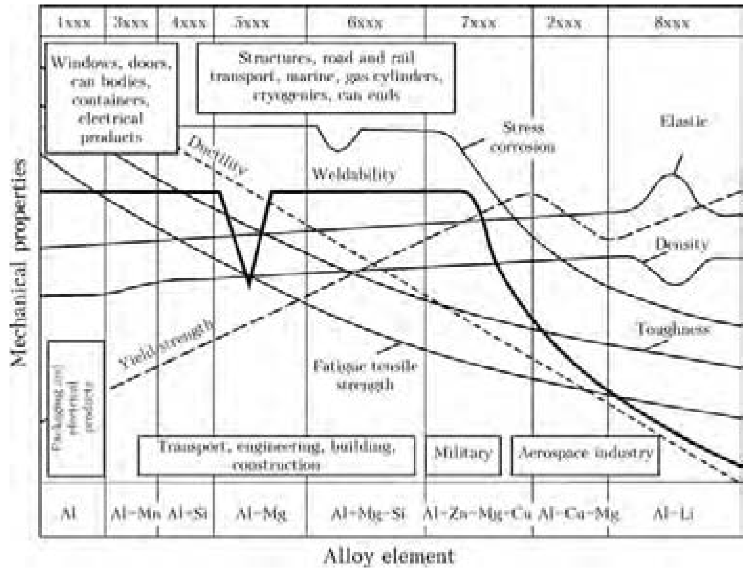

Figure 1. Mechanical properties of aluminium alloys

cally while some are weldable [11]. The chemical composition is usually copper and some other possible elements, like magnesium, manganese and silicon. They comprise high strength products that are usually typical of the aviation industry (2024 alloy). In the industry they are expected to meet high engineering standards due to high safety requirements. These requirements make the 2xxx series expensive. However, the alloys are also used in the manufacture of truck bodies (2014 alloy); 2011, 2017 and 2117 alloys are extensively used for fasteners and screw machine stock. Under naturally aged T4 condition, the 2xxx series alloys have similar mechanical properties as mild steel, with a proof strength of about 250 MPa and an ultimate tensile strength of around 400 MPa. They also have good ductility. When T6 conditioning is used, the proof strength gets up to 375 MPa and the ultimate tensile strength can get up to 450 MPa. This, in turn, lowers ductility [11]. Moreover, they are generally painted or clad to increase their corrosion resistance. Succinctly, the 2xxx series alloys are used for the construction of aircraft internal and external structures, internal railroad car structural members, structural beams of heavy dump and tank trucks and trailer trucks, and the fuel tanks and booster rockets of space shuttles [10].

The 7xxx series includes the Al–Zn alloys with magnesium to control the ageing process. The alloy group possesses very high strength in the high toughness versions. They are also heat treatable with an ultimate tensile strength range of 220–610 MPa. They can be mechanically joined and, with selected welding method like pulsed MIG process, they are weldable. Some 7xxx alloys content copper to yield the highest strength in the series. However, these alloys are not commercially weldable (Figure 1). The weldability reduces as the copper content increases [1–3]. Thus, in commercial applications they are mechanically joined, e.g. by riveting.

The 7xxx alloys are mainly used when fracture critical design concepts are important, e.g. the Foresmo Bridge in northern Norway. Al–Mg alloys are used for building the girders system. Another main application is in the aircraft industry [10]. They have poor corrosion resistance compared to, for example, the 5xxx series and are thus clad in many applications. They are used for critical aircraft wing structures of integrally stiffened aluminium extrusions and long-length drill pipes, and premium forged aircraft parts are made from 7175-T736 (T74) alloy [10].

The 8xxx series includes alloys with aluminium and other elements such as iron, nickel and lithium (not presented in Table 2). These elements provide a specific property to the alloy, e.g. nickel and iron yield strength to the alloy with almost no loss to electrical conductivity [10]. The high strength members of the series mainly consist of lithium and copper. The lithium proportion is higher than that of copper. The relatively recently developed Al–Li alloys 8090, 8091 and 8093 are also included in the series. Lithium has lower density than aluminium and relatively high solubility. Thus, it can be alloyed with aluminium in sufficient quantities. A significant reduction in density (usually about 10 % less than other aluminium alloys) is attainable. The resulting alloys have increased stiffness, and they also respond to age-hardening. Some of the series alloys are heat treatable [12]. They are therefore referred to as special alloys and have high conductivity, strength (tensile strength of 110–515 MPa [9]) and hardness. These alloys are used in the aviation industries (8090, 8091). The Al–Ni–Fe alloy 8001 is used in nuclear power generation for applications demanding resistance to aqueous corrosion at elevated temperatures and pressures. The alloy 8017 is used for electrical conduction [10].

Weldability of high-strength aluminium alloys. The increasing industrial need for aluminium alloys has resulted in profuse research on how to weld the new alloys. There are more ranges of applicable welding processes available on the market. Based on studies it can be stated that:

• within the scope of manufacturing technology, 94 % of alloys can be welded and over 50 % have optimal weldability;

• industrially weldable thickness range is 0.1–450 mm (the latter, exceptional case, in a single pass by means of electron beam welding (EBW));

• high welding speeds are attainable with reduced thicknesses (0.8–3.0 mm), for example, the laser welding of butt joints, varying between 5 and 3 m/min;

• metallurgical problems caused by welding heat input are present with all fusion methods, but reduced in the concentrated energy processes, where heat input is more precise and hence the HAZ is less extensive. FSW produces a low level of metallurgical disturbance;

• with concentrated energy processes, the presence of the Al_2O_3 film on the surfaces undergoing welding does not compromise the quality of the weld. However, pre-weld cleaning is encouraged;

• both EBW and FSW can be conducted without the use of gas to protect the weld pool from oxidation;

• traditional methods give inferior mechanical properties with respect to those of the corresponding base materials. The decrease varies from 20 to 35 % and is highly influenced by the metallurgical state of the base material. Particularly, an insignificant or even zero reduction is only found with the FSW process, which is, at the same time, the only welding process offering fatigue characteristics of butt joints that are entirely comparable to the base metal in the as-welded condition;

• generally all fusion welding methods, with the exception of FSW, give welds affected by widespread porosity;

• generally, and considering similar sized welding equipment, laser and FSW technologies involve up to 10 times higher investments than traditional technologies, but the level of productivity is decidedly superior. Currently, large scale of the aluminium alloy structural components welded by FSW have at least 10 % lower costs compared to those welded by MIG process [13].

Work preparation. The successful welding of HSA is very dependent on the work preparation due to the extra consideration necessary for welding aluminium compared to steel. It depends on using a suitable weld-

Table 3. Work preparation guide [4, 9, 14, 15]

Consideration	Precautions
Stress in weld	Avoid sudden changes in thickness as they act as stress raisers in the weld. It is better to taper a section in the joint if it is to be joined with a thinner section Ensure a good fit-up prior to welding. Aluminium is intolerant of poor fit-up and joints should have the smallest gap possible to allow the penetration of the filler into the joint. In a general fit-up, gaps of more than 1.5 mm are not acceptable. Larger gaps are easy to fill in steel but will introduce excessive stresses in aluminium due to thermal contraction. This will compromise the life of the weld Ensure a good alignment of the joint prior to welding. A misaligned weld will introduce bending stresses, which will also shorten the life of the weld Make sure that the joint preparation is suitable for the thickness of the material and complies with the drawing
Conditions for good quality welds	Make sure that the ambient conditions are suitable for welding. Aluminium is very sensitive to hydrogen contamination, so that any moisture will result in defective welds due to porosity. Welding outdoors is particularly risky as condensation can form on the joint during cold weather or the component may be left out in the rain. If welding is to be carried out during humid periods, moderate preheating may be usefully applied to prevent hydrogen porosity. Even if the joint is dry, the risk of draughts destroying the gas shield must be considered. Welding of aluminium is best carried out in a dedicated warm, dry, draught-free area indoors
Pre-weld cleaning of joint	Aluminium is very intolerant of contamination in the joint. Cleaning should start with a wipe by a clean cloth soaked in a solvent such as acetone to remove oil and grease from the joint area and 25 mm over both sides of the joint. All aluminium products have a very thin layer of oxide on the surface. This melts at about 2060 °C [4, 14] compared with 660 °C [9] for pure aluminium. This oxide must be removed after degreasing and before welding by mechanical cleaning with a stainless steel wire brush, which is reserved for aluminium use only. A grinding disk must not be used as these are made from corundum (aluminium oxide) and will deposit particles in the surface. This is precisely the material that cleaning intends to remove. The weld should preferably be made immediately after cleaning, but welding within 3 h of cleaning is acceptable
Suitability of welding consumables	Welding is normally carried out using argon or mixture of argon and helium, and the purity of these gases is important. A minimum purity of 99.995 % is required. Wire for MIG welding is normally supplied clean enough and it is sufficient to always ensure that the spool is preferably removed from the welding machine and placed in a clean plastic bag overnight or at least covered to keep it clean

Table 4. Shielding gases for MIG welding of aluminium [16]

Metal transfer mode	Shielding gas	Characteristics
Spray	100 % Ar	Best metal transfer and arc stability, least spatter, good cleaning action
	Ar + 65 % He	Higher heat input than in 100 % Ar, improved fusion characteristics on thicker material, minimised porosity
	Ar + 75 % He	Highest heat input, minimised porosity, least cleaning action
Short circuiting	Ar or Ar + He	Ar satisfactory on sheet metal, Ar + He preferred for thicker base materials

ing process, storage, handling and workpiece preparation as well as applying a practically acceptable joint design [1].

The workpiece to be joined with the pulsed MIG process involves joint preparation which is imperative to ensure quality welds. Based on the thickness of the workpiece, the joints need to be bevelled and in some cases a root back-up must be applied. It is important to clean the joint surface to remove the thin oxide layer (Al_2O_3). The removal can be done by mechanical abrasion processes like brushing with stainless steel brushes or by chemical etching. The Al_2O_3 layer regenerates itself when scratched. It is responsible for the corrosion resistance in aluminium alloys [14] and also for the arc instability problem because it is electrically non-conductive. Al_2O_3 is hygroscopic and it is usually found hydrated. The melting temperature is 2060 °C [4, 14] which is high when compared to the melting temperature range of 476–657 °C of the 7xxx series alloys [9]. A work preparation guide is presented in Table 3.

Shielding gas. The primary function of shielding gas is to protect the weld metal from the atmosphere because heated metal (around the melting point) usually exhibits a tendency to react with the atmosphere to form oxides and nitrides. For aluminium it easily reacts with oxygen at room temperatures. In selecting the shielding gas, the criteria that should be met are as follows [4, 16–18]:

- gas must be able to generate plasma and stable arc mechanism and characteristics;
- it should provide smooth detachment of molten metal from the wire and fulfil the desired mode of metal transfer;
- it should protect the welding head (in the arc immediate vicinity), molten pool and wire tip from oxidation;
- it should help to attain good penetration and good bead profile;
- it should not be detrimental to the welding speed of the process;
- it should prevent undercutting tendencies;
- it should limit post-weld cleaning;
- it should not be detrimental to the weld metal mechanical properties.

The recommended shielding gas for pulsed MIG welding of 7xxx aluminium is argon [1, 17] at flow rate of about 20 l/min. A mixture of argon and helium can also be used and even helium alone. Helium increases weld penetration, offers higher arc energy and, thus, an increased deposition rate [1, 19]. When the section is lower than 50 mm, helium should be used [4]. More details can be seen in Table 4.

Welding defects in HSA and UHSA. The welding of aluminium is rather critical despite the fact that it has a lower melting point compared to steel. The welding of aluminium is critical because of the following considerations [6, 18]:

- stable surface oxide needs to be eliminated before welding;
- presence of residual stresses causes weld cracking due to the high thermal expansion coefficient of aluminium;
- high heat conductivity of aluminium implies that great heat is required to achieve welds, whereas high heat input increases the possibility of distortion and cracking;
- high shrinkage rates on solidification enhance cracking;
- high solubility of hydrogen in molten aluminium causes porosity;
- general susceptibility of the 2xxx, 7xxx and 8xxx series to weld cracking.

Applicable major welding defects in HSA series include hot cracking, porosity, joint softening, not recoverable on post-weld ageing, poor weld zone ductility (HAZ degradation) and the susceptibility of the joint to stress corrosion cracking (Table 5).

Experimental set-up. The experiment was carried out using a robotised pulsed MIG welding machine. The schematics of the MIG welding process are presented in Figure 2.

The robot movement was programmed and some test sample welds were made, after which alloy 7025-T6 was welded. Many different welds were made, and the weld parameters were varied to study the effect of heat input on properties of the weld metal. Furthermore, the effect of the welding speed was studied.

The MIG torch used was Fronius Robacta 5000 360 (max 500 A). The torch was connected to the Motorman (EA1900N) robot. The robot has 6 axes and can attain an accuracy of up to ±0.06 mm. A torch angle of 10° pushing weld direction was used to allow for the purging of the weld area ahead of the arc. The

Table 5. Defects in aluminium welds and their prevention [11, 15, 18, 20]

Defect	Cause	Remedy
Oxide inclusions	Insufficient cleaning of the joint Oxide layer on welding wire or filler rods Sharp edges on the joint groove	Thoroughly wire brush before welding and after each pass, then wipe clean Clean wire and rods by abrading with stainless steel wool or «Scotchbrite» Use fresh spool of wire Break sharp edges in weld preparation
Porosity in weld	Inadequate shielding Dye penetrants, lubricants Welding current too high Contaminated shielding gas Incorrect torch angle Travel speed too high Contaminated wire or rods Moisture	Increase gas flow Eliminate draughts Reduce electrode extension Remove any defects fully Clean surfaces with a solvent Keep lubricants away from the weld area Reduce current and refer to the weld procedure Check gas hoses for loose connections or damage Check torch coolant to ensure no leaks Replace gas cylinders Use correct angle and refer to the weld procedure Apply correct speed and refer to the weld procedure Clean wire or rods with solvent Preheat and clean the surface
Porosity in fusion zone	Hydrogen in the base metal	Improve the degassing practice Reduce sodium additions Apply 100 % He shielding
Cold cracking	High joint restraint	Slacken holding clamps Preheating
Hot cracking	Excessive dilution by parent Interpass temperature too high	Reduce welding current Add more filler wire Reduce welding current Cool between passes and sequence welds
Undercutting	Welding current too high Travel speed too high and insufficient filler metal Arc length too long	Reduce current Reduce speed and refer to the weld procedure, add more filler metal Reduce arc length
Lacks of fusion	Welding current too low Travel speed too high Poor joint preparation Incorrect torch angle	Increase current and refer to the weld procedure Reduce travel speed, and refer to the weld procedure Improve joint preparation Apply correct torch angle, and refer to the weld procedure
Crater cracking	Improper breaking of arc	Reduce arc current gradually Use «Crater fill» control if available. «Back weld» over last 25 mm of the bead
Overlap	Slow travel speed Welding current too low Too much filler metal Incorrect torch angle	Increase speed and refer to the weld procedure Increase current Reduce filler metal addition Change torch angle
Drop through	Slow travel speed Welding current too high Joint gap too wide Too much heat built up in part	Increase travel speed Decrease welding current Reduce gap and improve the fit-up Reduce interpass temperature

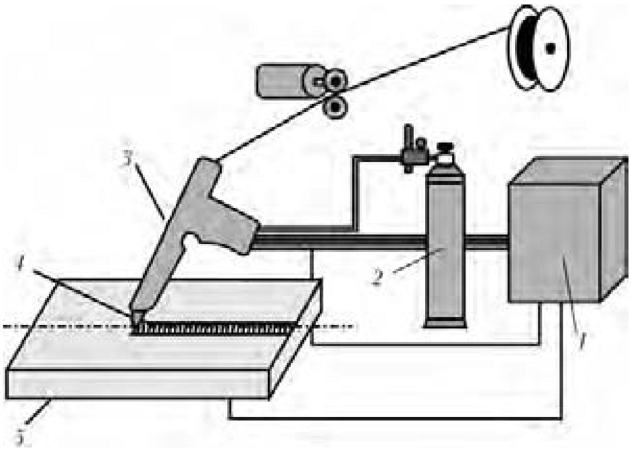

Figure 2. Schematics of MIG welding process: *1* — power source; *2* — shielding gas; *3* — MIG torch; *4* — filler wire; *5* — aluminium workpiece

filler wire extension was 2 mm, and the nozzle-to-workpiece distance (stick-out length) was 18 mm. The shielding gas used was 99.995 % argon and the filler wire was 4043 aluminium. The workpiece was a 5 mm thick plate with an area of 100 × 250 mm. The samples were bead-on-plate welds, so there was no bevelling. However, the joints were cleaned mechanically by using a stainless steel bristle brush reserved for aluminium only.

Many experimental trials were performed, for which 6 different samples of 7025-T6 alloy were selected. The first three samples (A, B and C) had the same feed rate so as to investigate the effect of the welding speed (10, 20 and 30 mm/s). The other three samples (D, E and F) had approximately the same heat input to investigate the effect of constant heat input on the weld. The pulse current frequency was approximately 250 Hz in each weld.

For samples A–C, the feed rate was constant at 10 m/min, and the heat input varied. Heat input Q for all samples was calculated as [21]

$$Q = \frac{VI{\cdot}60}{1000S} \cdot 0.8, \qquad (1)$$

where Q is the heat input, kJ/mm; V is the voltage, V; I is the current, A; S is the welding speed, mm/min; 0.8 is the efficiency of the pulsed MIG process.

For samples D–F, heat input was approximately constant and the feed rates were selected as 10, 12 and 14 m/min, respectively.

The base material was a 5 mm thick 7025-T6 plate, and the welding wire was ER 4043 (Table 6). The typical mechanical properties of the wire include the yield stress of 55 MPa, tensile strength of 165 MPa and an elongation of 18 %. The shielding gas was 99.995 % argon and it was supplied through the MIG torch to protect the weld pool from the atmosphere, because heated metal (around the melting point) usually exhibits a tendency to react with the atmosphere to form oxides and nitrides. For aluminium it easily reacts with oxygen at room temperatures. The recommended shielding gas for pulsed MIG welding 7xxx series aluminium is argon [17].

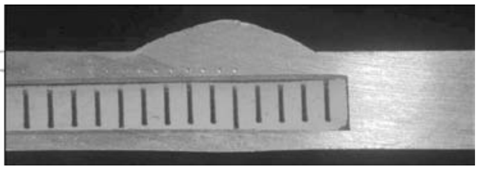

Figure 3. Hardness testing on a weld sample

The hardness testing experiment of the welds was done on a Vickers hardness machine. The test method involved the indentation of the test workpiece with a diamond indenter in the form of right pyramid with a square base and angle of 136° between opposite faces; subjected to a weight of 1–100 kg. The full load was normally applied for 10–15 s. The two diagonals of the indentation made on the surface of the material after the removal of the load were measured using a microscope and their averages calculated [22].

This test was carried out by a 3 kg weight indentation of the diamond tool tip on the prepared weld cross-section. The weight can be varied for different materials, but 3 kg was sufficient because aluminium is relatively soft and 3 kg is enough to create an indentation. Moreover, it is important that the weight is low enough for the aluminium test piece to resist it. The indentations were done at about 1 mm from the weld surface in a row (Figure 3).

The distance between each indentation was 0.7 mm. The shape of the indentation resembled a rhombus. The depth of the indents depended on the material hardness. The dimension of the diagonals of an indentation was measured and the average value from the diagonals was looked up from the hardness table of *HV*3 to determine the hardness value. The values were then plotted against the distance of each indentation from the weld centreline.

Results and discussions. *Effect of heat input on HSA*. Micro- and macrostructure, as well as weld appearance on samples A–C, are presented in Figures 4–6. The picture of each sample shows the microstructure using an ×8 magnification lens for analysing the unmixed zone (UZ), partially melted zone (PMZ),

Table 6. Chemical composition of base metal and filler wire used, wt.%

Metal	Al	Be	Cr	Cu	Fe	Mg	Mn	Si	Ti	Zn	Other each	Total
7025	91.5	–	0.30	0.10	0.40	1.50	0.60	0.30	0.10	5.0	0.05	0.15
ER 4043	–	0.0001	–	0.01	0.20	0.01	0.01	4.80	0.02	0.01	–	–

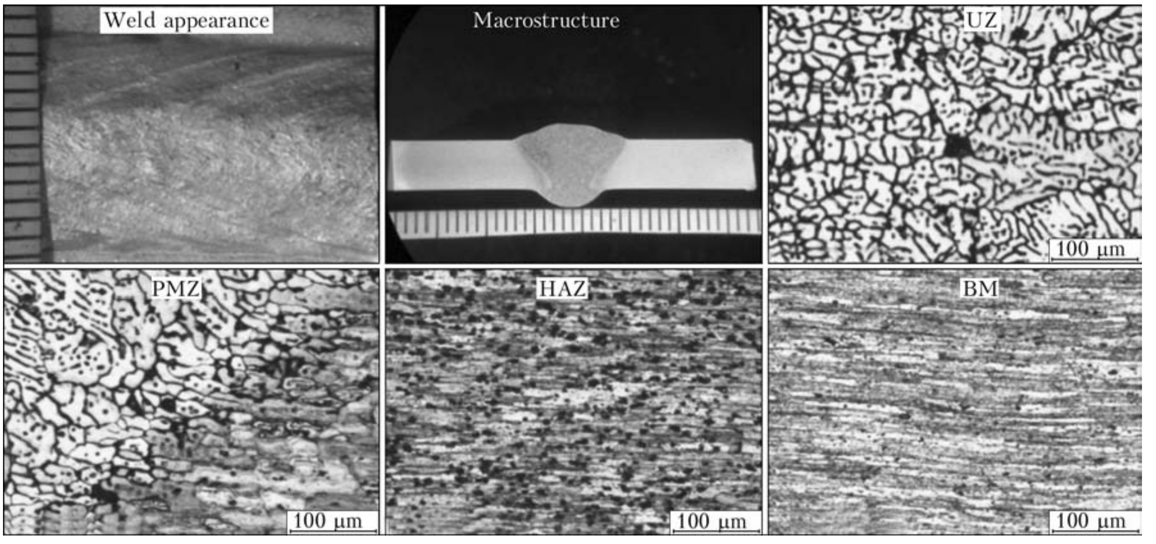

Figure 4. Experimental results for sample A welded at $v_{w.f}$ = 10 m/min, v_w = 10 mm/s, Q = 0.318 J/mm, U = 20.1 V and I = 198 A

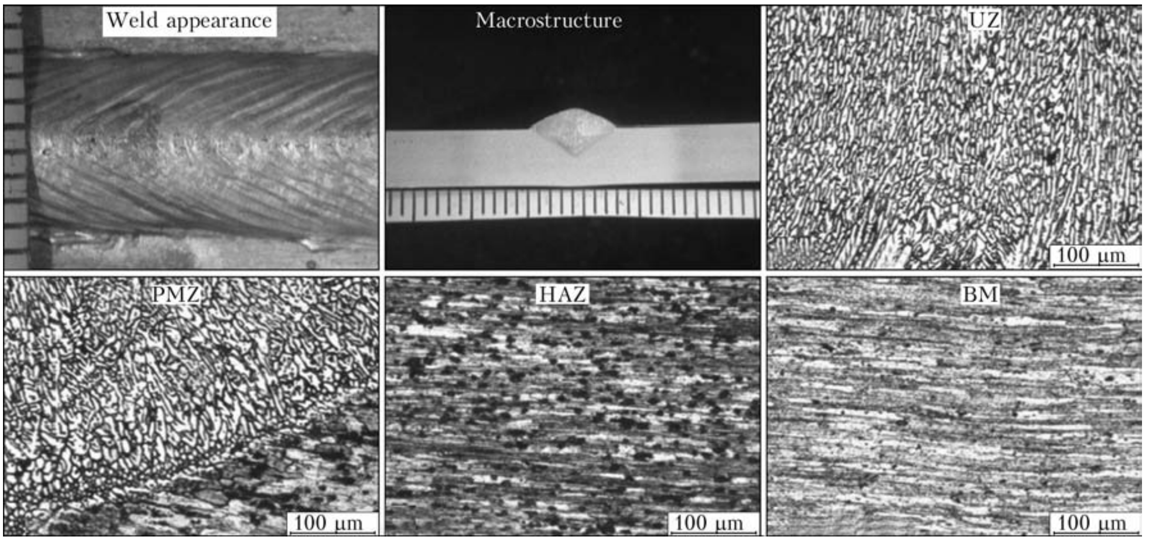

Figure 5. Experimental results for sample B at $v_{w.f}$ = 10 m/min, v_w = 25 mm/s, Q = 0.127 J/mm, U = 19.4 V and I = 205 A

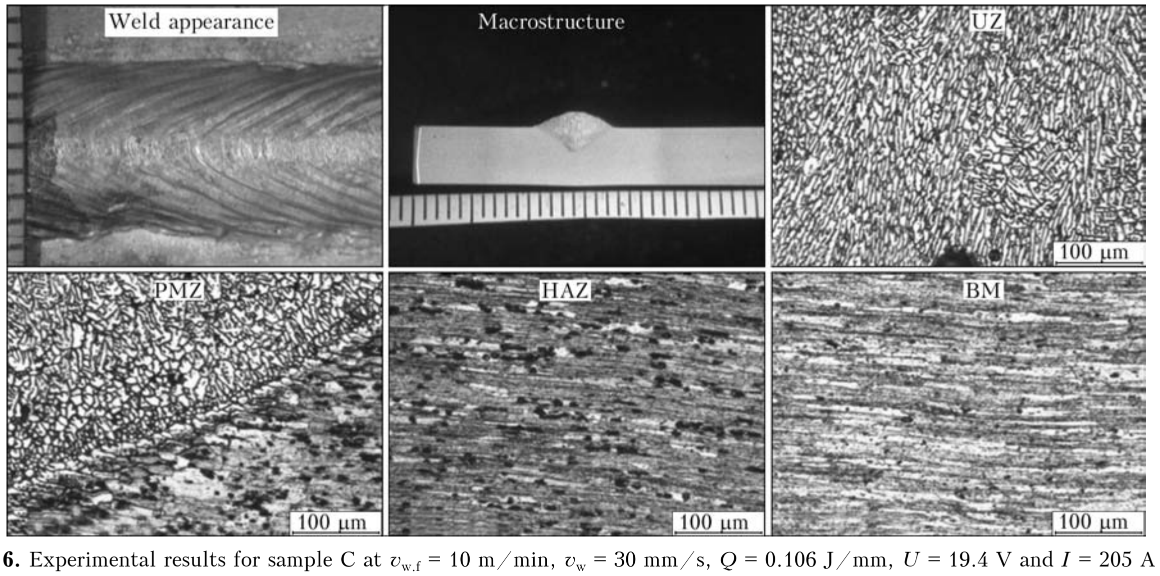

Figure 6. Experimental results for sample C at $v_{w.f}$ = 10 m/min, v_w = 30 mm/s, Q = 0.106 J/mm, U = 19.4 V and I = 205 A

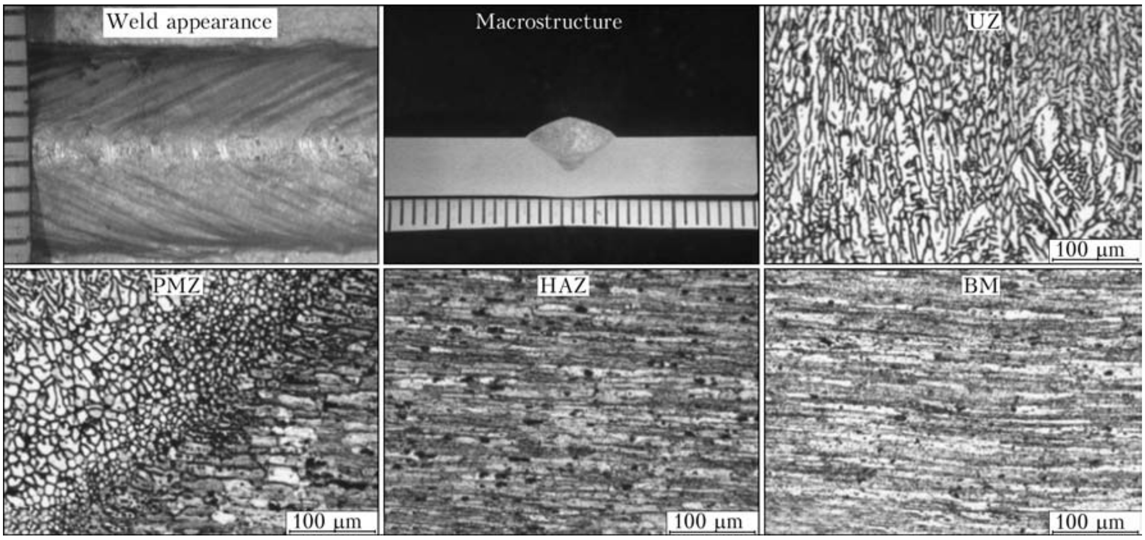

Figure 7. Experimental results for sample D at $v_{w.f}$ = 10 m/min, v_w = 20 mm/s, Q = 0.16 J/mm, U = 19.8 V and I = 202 A

heat-affected zone (HAZ) and base metal (BM). The transition around the weld interface is of great significance. The picture shows how the grains have been transformed, from which inferences can be made as to the mechanical properties of the weld samples.

Comparing samples A, B and C (see Figures 4–6), it can be seen that the grain sizes around the weld interface are small when heat input is low, and vice versa. Furthermore, the transition flow of cells at the interface as it moves from the UZ to the HAZ is smoother with higher heat input where the grain sizes are bigger. With lower heat input as in sample C (see Figure 6) the transition is not as smooth, so the interface is distinct. Heat input is inversely related to the welding speed. When the welding speed increases, heat input reduces. The higher the heat input, the higher the cooling rate. A high cooling rate allows epitaxial growth to occur and also for the cells to grow large, as seen by comparing sample A to samples B and C. In sample A, the HAZ is about 17 mm from the weld centreline, which is the greatest distance of the three samples (see Figure 4). Thus, it can be said that the higher the heat input, the wider the HAZ.

The grains of UZ in sample C compared to B and A are very fine, which shows that low heat input in A and B is insufficient to melt the pool and penetrate the weld. The high heat input and high welding speed caused high heat energy on the weld in sample C, which makes the weld bead large with a wider root.

Sample C has fine grains compared to B and A, which shows that with high heat input and welding speed there is higher nucleation. In sample C, the grain growth is low compared to A and B because aluminium dissipates heat relatively fast through heat sinks; low heat input means that the high conductivity of aluminium strongly affects the weld microstructure (sample C cools fast).

By comparing the results from samples D, E and F presented in Figures 7–9 it can be noted that keeping the heat input relatively constant but varying the welding speed causes changes in the microstructure. As the welding speed and the wire feed rate increase,

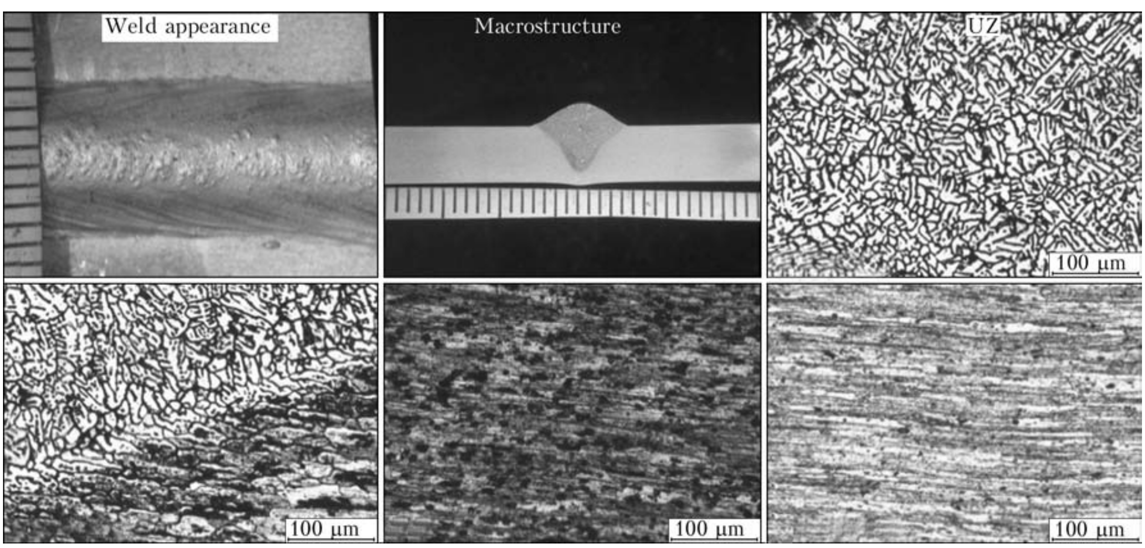

Figure 8. Experimental results for sample E at $v_{w.f}$ = 12 m/min, v_w = 24 mm/s, Q = 0.163 J/mm, U = 20.3 V and I = 241 A

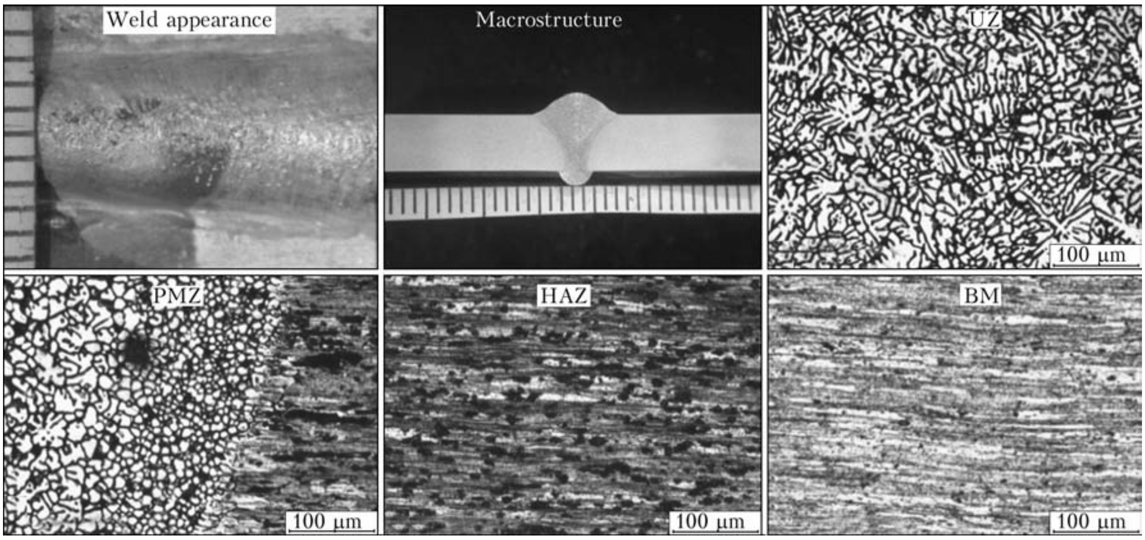

Figure 9. Experimental results for sample F at $v_{w.f}$ = 14 m/min, v_w = 28.8 mm/s, Q = 0.158 J/mm, U = 20.5 V and I = 278 A

also the grain sizes increase. Furthermore, the increased welding speed gives lower nucleation and coarser transitions of grains around the weld interface, which is similar to the effect of heat input in 7025-T6 aluminium welds.

Samples D, E and F indicate that the higher the wire feed rate, the deeper the penetration. Sample C has a constant feed rate with A and B but the grain transition at the weld interface between the UZ and the HAZ is very sharp. This may be a possible failure point as the cells are not as interlocked as in sample B. Sample A shows that the longer the solidification time, the bigger the size of the dendrite [23].

The grains are equiaxed with dendrites within the grains. Fine grain sizes appear when heat input is low, and coarse grain sizes when heat input is high. For example, the UZ in Figure 8 has fine grains due to the low heat input of 0.163 kJ/mm, whereas the UZ in Figure 4 has coarse grains due to high heat input of 0.318 kJ/mm. The grain size variations in the UZ in Figures 4–9 are mainly due to the amount of heat input, since high heat input means a high cooling rate.

A faster welding speed allows narrow welds even with lower heat input (comparing samples A–F). Sample F seems to be the best weld with a narrow bead, narrow HAZ and complete penetration. On the other hand, oxidation occurred on the surface. At a constant welding speed, high heat input increases the weld bead size and HAZ size. The PMZ shows epitaxial growth, which indicates that new grains had nucleated on the heterogeneous sites at the weld interface. There is a random orientation between the base metal grains and weld grains.

As can be seen from samples A–F, since the ratio of 7025-T6 alloy temperature gradient G to the growth rate R decreases from the weld interface towards the centre line, the solidification modes have changed from planar to cellular, to columnar dendrite and equiaxed dendrite across the weld interface . The ratio G/R determines the solidification modes found in the microstructure. Sample C has the smallest grain size in the UZ. Thus, it can be concluded that it has the highest strength and toughness as the Hall–Petch effect predicts that both strength and toughness increase as the grain sizes reduce [24, 25]. Sample F shows that complete weld penetration can be achieved with minimal heat input if other weld data are set correctly.

Weld defects such as porosity and oxidation were found on the welds. Porosity could be due to gas entrapment during welding, whereas oxidation could be due to poor shielding gas covering (the weld pool has contact with atmospheric air).

Hardness of HSA welded joints (7025-T6). The hardness tests of samples A–C are presented in Figure 10, where the plots for samples A, B and C are combined on the same graph. The vertical line, labelled WI, denotes the weld interface. The points on the graph curve indicate the distance of each indentation point from the weld centreline on the horizontal axis and the hardness value when traced on the vertical axis. The graph also shows the weld zones, HAZ and BM. Sample C has the lowest heat input of 0.106 kJ/mm resulting in a high hardness profile, sample B — relatively higher heat input of 0.127 kJ/mm resulting in a lower hardness profile than sample C, and sample A — the highest heat input of 0.318 kJ/mm resulting in the lowest hardness profile.

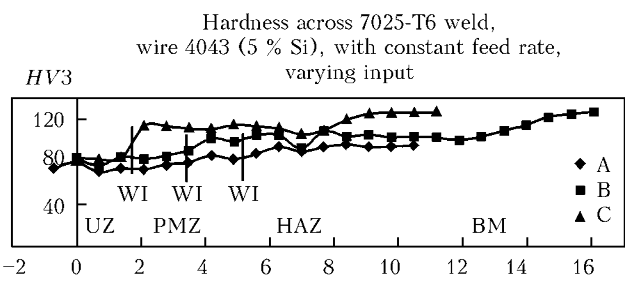

Figure 10. Hardness distribution for samples welded with varying heat input: 0.106 (C), 0.127 (B), 0.318 (A) kJ/mm

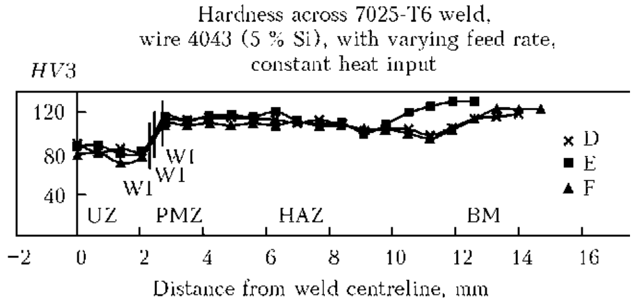

Figure 11. Hardness distribution for samples welded with relatively constant heat input of about 0.16 kJ/mm

Sample C also has the highest hardness at the WI, thus, implying that high heat input allows for high hardness of the WI, due to solution hardening during welding. High heat input causes solubility and thereby higher hardening through the solidification process. It can also be said that the higher the heat input, the wider the weld bead and the further away from the weld centreline is the WI. The hardness test also shows this with relatively constant heat input. The hardness pattern of samples D, E and F are similar, but E exhibits small variation. The hardness around 3 mm away from the weld centreline shows a rapid increase in the value from the previous point (around 2 mm from the weld centreline). This is due to the closeness of the WI. From samples D, E and F it can be seen that for 7025-T6 weld, hardness reduces in the weld zone and increases towards the base material. The hardness graph presents half of the symmetric welds. At the WI it can be said that the hardness values of D, E and F samples are relatively identical. This implies that at constant heat input, the hardness profile of 7025-T6 aluminium alloy remains the same.

The hardness tests of samples D, E and F, presented in Figure 11, show that the hardness profiles for the three samples are relatively similar. The WI range is within 0.5 mm as a result of a relatively constant heat input. The labelling and description of the graph is the same as for samples A–C.

CONCLUSIONS

1. The study showed that in 7025-T6 aluminium alloys the grain size reduces as the heat input reduces. The transition of cells from the UZ to HAZ is smoother with higher heat input. At constant heat input the grain size increases when wire feed rate, welding speed and current increase simultaneously but the hardness remains relatively constant. When heat input is high, the HAZ is wider, nucleation is lower, and the grains around the weld interface are coarser.

2. In 7025-T6 aluminium alloy, high heat input results in a low hardness profile but the hardness of the UZ is the same in all the selected samples. The higher the heat input, the wider the weld bead, the further away is the weld interface and the deeper the weld penetration. The longer the solidification time, the larger the dendrites and a high cooling rate allows for epitaxial cell formation. The 7025-T6 alloy, like other high-strength aluminium alloys, experiences HAZ softening but can be restored by postweld heat treatment.

1. Yeomans, S.R. (1990) Successful welding of aluminium and its alloys. *Australian Welding J.*, 35(**4**), 20–24.
2. Graeve, I.D., Hirsch, J. (2010) 7xxx series alloys. *http*://aluminium.matter.org.uk/content/html/eng/default.asp?catid=214&pageid=2144417086
3. Dickerson, P.B., Irving, B. (1992) Welding aluminium: It's not as difficult as it sounds. *Welding J.*, 71(**4**), 45–50.
4. Mathers, G. (2002) *The welding of aluminium and its alloys*. Boca Raton: CRC Press; Woodhead Publ.
5. Maurice, S. (1997) *Aluminum structures*: Handbook of structural engineering. 2nd ed. CRC Press.
6. Campbell, F.C. (2006) *Manufacturing technology for aerospace structural materials*. Amsterdam; San Diego: Elsevier.
7. (2008) *ASM Handbook*. Vol. 15: Casting. Materials Park: ASM Int.
8. Kopeliovich, D. (2009) Classification of aluminum alloys. In: *Substances and technology*.
9. (2010) *MatWeb — The Online Materials Information Resource*.
10. Kaufman, G.J. (2000) *Applications for aluminum alloys and tempers*. ASM Int.
11. John, D. (1999) Heat-treatable alloys. In: *Aluminium design and construction*. New York: Taylor & Francis, 301.
12. *Aluminum alloys and temper designations 101*. Dayco Ind., 1–5.
13. Volpone, L.M., Mueller, S. (2008) Joints in light alloys today: the boundaries of possibility. *Welding Int.*, 22(**9**), 597–609.
14. George, E.T., MacKenzie, D.S. (2003) *Handbook of aluminum: Physical metallurgy and processes*. New York: Marcel Dekker.
15. Renshaw, M. (2004) The welding of aluminium castings. In: *Aluminium — light strong and beautiful*. A.F.o.S. Africa, 11–13.
16. (2008) Choosing shielding gases for gas metal-arc welding. *Welding J.*, 87(**4**), 32–34.
17. Boughton, P., Matani, T.M. (1967) Two years of pulsed arc welding. *Welding and Metal Fabr.*, Oct., 410–420.
18. Olson, D.L. (1993) *Welding, brazing, and soldering*: ASM handbook. Metals Park: ASM Int.
19. Blewett, R.V. (1991) Welding aluminium and its alloys. *Welding and Metal Fabr.*, Oct., 5.
20. Ba Ruizhang, G.S. (2004) Welding of aluminum-lithium alloy with a high power continuous wave Nd:YAG laser. *IIW Doc. IV-866–04*.
21. Hirata, Y. (2003) Pulsed arc welding. *Welding Int.*, 17(**2**), 98–115.
22. Chandler, H. (1999) *Hardness testing*. Materials Park: ASM Int.
23. Kou, S. (2003) *Welding metallurgy*. Hoboken: Wiley-Intersci.
24. Sato, Y.S., Urata, M., Kokawa, H. et al. (2003) Hall–Petch relationship in friction stir welds of equal channel angular-pressed aluminium alloys. *Materials Sci. and Eng. A*, 354(**1/2**), 298–305.
25. Vander Voort, G.F., (2004) *Metallography and microstructures*. Materials Park: ASM Int.